Leukemia (2013), 1–4

www.nature.com/leu

LETTER TO THE EDITOR

Specificity and mechanism-of-action of the JAK2 tyrosine kinase inhibitors ruxolitinib and SAR302503 (TG101348)

Leukemia advance online publication, 19 July 2013; doi:10.1038/leu.2013.205

Activating point mutations in the JAK2 kinase were identified in BCR-ABL-negative myeloproliferative neoplasms, including polycythemia vera, essential thrombocythemia and primary myelofibrosis (MF).[1,2] This encouraged the development of several small-molecule JAK2 tyrosine kinase inhibitors,[3] of which ruxolitinib (formerly known as INCB018424) was approved by the US Food and Drug Administration for the treatment of patients with intermediate or high-risk MF, including primary MF, post-polycythemia vera MF and post-essential thrombocythemia MF.[4,5] Another JAK2 inhibitor, SAR302503 (formerly known as TG101348), is in advanced clinical trials.[6,7] Both drugs inhibit JAK2 kinase activity *in vitro* and JAK2-dependent proliferation of cell lines with IC_{50} values in the low nanomolar concentration range.[8,9] Among the four kinases of the JAK family (JAK1, JAK2, JAK3 and TYK2), SAR302503 also inhibits JAK1, Tyk2 and JAK3, albeit with ~30-, ~100- and ~300-fold weaker efficiency than JAK2, respectively.[9] Ruxolitinib inhibits JAK1 and JAK2 equally well, and targets TYK2 >10-fold and JAK3 ~100-fold weaker.[8] As both drugs were only tested for inhibition of a few dozen unrelated kinases,[9,8] accounting for only a small portion of the 518 human kinases, comprehensive data on their specificity are missing. In addition, no structural data of ruxolitinib or SAR302503 bound to the JAK2 kinase domain that would reveal their binding modes and molecular mechanism-of-action are available. Of note, ruxolitinib is the only FDA-approved kinase inhibitor for which no co-crystal structure with its target kinase has been published.[10] Here, we present a near-kinome-wide survey of the specificity of ruxolitinib and SAR302503 and determine their binding modes to the JAK2 kinase domain by extensive sampling using molecular dynamics (MD) simulations.

For specificity testing, we used a panel consisting of 368 recombinant human kinases (including 70 kinase mutants relevant to human disease), thereby covering ~60% of the human kinome. Inhibition of the kinase activity *in vitro* was assayed for both drugs in parallel at a concentration of 1.0 μM. Ruxolitinib inhibited the activity of 33 kinases (including 11 kinase mutants) by ⩾50%, whereas 54 kinases (including 14 kinase mutants) were inhibited by SAR302503 (Table 1a and Supplementary Data). Eleven and 14 kinases (including 2 and 4 kinase mutants, respectively) were inhibited by ruxolitinib and SAR302503, respectively, by ⩾80% (Table 1a). We subsequently determined the IC_{50} values for kinases that showed profound inhibition in the tested panel. We concentrated on known oncogenes and/or validated drug targets in cancer and other diseases. These included the receptor tyrosine kinases ALK, RET, TRK-B, the cytoplasmic tyrosine kinases ACK1, FAK, LCK and the serine/threonine kinase JNK1. Ruxolitinib strongly inhibited TRK-B (IC_{50} = 11 nM), as well as ACK1, ALK and RET with IC_{50} values below 300 nM. SAR302503 inhibited LCK and RET with IC_{50} values ~500 nM, and ACK1, FAK and JNK1 with IC_{50} values ~200 nM (Table 1b) in addition to the previously described inhibition of FLT3 and BCR-ABL.[9,11] We were intrigued when we found LRRK2 and several of its pathogenic mutants, which are common causes of familial Parkinson's disease,[12] to be profoundly inhibited by both JAK2 inhibitors (Table 1a). We then used *in vitro* kinase inhibition assays for LRRK2 and monitored the cellular phosphorylation of LRRK2 at Ser-910/935 as a pharmacodynamic marker of LRRK2 kinase activity. LRRK2 kinase activity was inhibited *in vitro* with IC_{50} values 820 nM and 1.8 μM for ruxolitinib and SAR302503, respectively (Table 1b), but both drugs were not able to strongly inhibit the LRRK2 phosphorylation at Ser-910/935 in cells (data not shown). SAR302503 inhibits a much larger number of off-target tyrosine kinases than ruxolitinib (31 vs 15, excluding the JAK kinases), whereas the number of off-target serine-/threonine kinases is similar for both drugs. The tyrosine kinases that are targeted by SAR302503, but not by ruxolitinib, include the SRC family kinases LCK and FGR, the T-cell kinase ITK, as well as the KIT and FLT3 receptor kinases, all of which are critical for hematopoietic cell signaling. In addition, SAR302503 targets kinases that are predominantly expressed in non-hematopoietic cells, such as PDGFR members and DDR2. Those are thought to contribute to the side-effect profile of BCR-ABL tyrosine kinase inhibitors. Based on these observations, one may speculate on a higher incidence of adverse events in patients treated with SAR302503, as compared with ruxolitinib.

The detailed knowledge of the binding mode of a kinase inhibitor at the atomic level is essential to understand its mechanism-of-action, interpret its specificity, predict and rationalize its resistance mechanisms, and suggest points of chemical derivatization for improved potency and specificity. To shed light on the binding mode of ruxolitinib and SAR302503 to JAK2, we carried out multiple runs of MD simulations (simulation protocols and analyses of MD trajectories are in the Supplementary Information). MD is a computational method to assess the structure and flexibility of proteins and their interactions with ligands. Notably, we performed simulations with explicit solvent and full flexibility of both JAK2 and inhibitor, that is, taking into account not only enthalpic but also entropic contributions of drug binding. It is important to note that MD simulations are significantly more accurate (albeit computationally more expensive) than the commonly used docking with rigid protein targets. Following a similar MD-based simulation protocol, we previously predicted the binding mode of a potent ATP-competitive inhibitor of the EphB4 tyrosine kinase, which is essentially identical to the subsequently determined crystal structure.[13] The MD simulations (cumulative sampling of 1.5 and 9.6 μs for ruxolitinib and SAR302503, respectively) suggest that both drugs inhibit JAK2 by a so-called type I binding, in which the inhibitor targets the ATP-binding site of the kinase in its active conformation and the DFG-motif at the base of the activation loop is in its inward-facing conformation.[14] Importantly, the analysis of the free-energy surface (Supplementary Figures S2 and S3) and displacement from the starting poses (Supplementary Figure S8) indicate that there are multiple poses, that is, multiple positions, orientations and/or conformations, of each of the two drugs in the ATP-binding site (Figure 1 and Supplementary Figures S4 and S7). The double-ring system (7H-pyrrolo[2,3-d]pyrimidin) of ruxolitinib is involved in two persistent hydrogen bonds with the so-called hinge region,

Accepted article preview online 4 July 2013

which is the sequence segment that connects the N-lobe to the C-lobe of the kinase domain (Figures 1a and b). These two key interactions are preserved during all simulations of ruxolitinib (Supplementary Figure S1). In contrast, the cyclopentane ring and propanenitrile, as well as the pyrazole ring, can vary their orientations with respect to the rigid double-ring system (Figure 1a and Supplementary Figures S2–S4).

Table 1. Target profile of ruxolitinib and SAR302503

a

Ruxolitinib		*SAR302503*	
Kinase	*% Inhibition at 1 μM*	*Kinase*	*% Inhibition at 1μM*
TYK2	100	JAK2	98
JAK2	99	TSF1	96
JAK1	97	DAPK3	96
JAK3	96	FGF-R1 V561M	94
TRK-B	94	ACV-R1	90
LTK	90	MUSK	88
TRK-C	88	ACK1	87
CAMK2A	86	FAK	86
LRRK2 G2019S	84	ACV-RL1	86
RET V804M	83	RET V804L	84
CAMK2D	80	DAPK1	84
RET V804L	78	TYK2	83
MEKK3	76	FLT3 ITD	83
ACK1	72	RET V804M	82
ROCK1	71	DAPK2	79
ALK	69	FLT3 D835Y	78
RET R813Q	67	PDGFR-beta	72
MEKK2	66	RET R813Q	72
DAPK3	66	JAK1	72
ROCK2	65	JNK3	69
LRRK2 wt	64	SAK	69
LRRK2 R1441C	62	JNK2	68
RET wt	61	RET wt	67
LRRK2 I2020T	60	RET M918T	67
RET R749T	57	RET Y791F	67
DAPK1	57	RET E762Q	66
RET M918T	57	NEK9	65
RET E762Q	57	PDGFR-alpha	65
RET Y791F	57	LCK	65
RET G691S	55	RET G691S	64
CSF1-R	55	RET R749T	64
PRKG2	55	TXK	63
DAPK2	51	FGF-R1 wt	62
		DDR2	61
		RET S891A	60
		ROS	60
		LRRK2 G2019S	59
		KIT V560G	59
		ITK	59
		JAK3	59
		JNK1	58
		TAOK2	57
		FGF-R2	57
		TGFB-R2	55
		TRK-A	54
		AXL	54
		SNF1LK2	54
		TRK-C	53
		Aurora-B	53
		PRKG2	52
		TRK-B	52
		FGR	52
		STK33	51
		ARK5	50

b

Kinase	*IC_{50}/nM*	
	Ruxolitinib	*SAR302503*
ACK1	230	170
ALK	290	3400
FAK	3500	160
JNK1	>10000	260
LCK	3600	500
RET	280	560
TRK-B	11	1200
LRRK2 wt	820	1800

(**a**) Both drugs were assayed at a concentration of 1 μM against a panel of 368 recombinant human kinases *in vitro* in duplicates (ProQinase assay panel). All kinases that are inhibited by more than 50% are shown in the table. (**b**) IC_{50} for inhibition of selected kinases were determined by 10 serial dilutions of the drugs in semi-log steps and calculated using Graphpad Prism. The raw data-set is presented as Supplementary Data.

Concerning SAR302503, the simulations suggest two main binding modes that, in contrast to ruxolitinib, even differ in the hydrogen bonds with the hinge region (Figure 1 and Supplementary Figure S7). As mentioned above, the binding modes of both drugs were obtained by taking into account full flexibility of both JAK2 and the drug, as well as solvent effects. Moreover, multiple long simulations were carried out to obtain statistically significant sampling. Therefore, our MD simulations offer a first reliable structural view on the possible binding modes of ruxolitinib and SAR302503 to JAK2. It is also not surprising that the binding mode of ruxolitinib proposed here differs strongly from the one reported recently by others, which was obtained by a much simpler computational protocol, that is, rigid protein docking,[15] and is not stable according to MD simulations (Supplementary Figure S4).

Mutation of the so-called gatekeeper residue in various kinases, such as the T315I mutation in BCR-ABL, is a common cause of resistance to kinase inhibitors in the clinical use.[10] Based on the results of our MD simulations, the hydrophobic pocket guarded by the gatekeeper residue (Met-929) is not involved in ruxolitinib and SAR302503 binding to the JAK2 kinase domain (Figure 1c). In addition, the gatekeeper residue in the identified off-target kinases of ruxolitinib and SAR302503 (Table 1) differs in size and hydrophobicity (mainly Met, Val, Thr, Phe or Leu). Together, this indicates that ruxolitinib and SAR302503 bindings are not influenced by the identity of the gatekeeper residue. This finding is in contrast to the kinases that are targeted by the BCR-ABL inhibitors imatinib, nilotinib and dasatinib, which almost exclusively contain threonine as a gatekeeper residue.[16] In line with these observations, a recent unbiased screen for ruxolitinib resistance mutations in a cell line model did not identify mutations of the JAK2 gatekeeper (Met-929).[15] *In vitro* inhibition assays with the JAK2 M929I gatekeeper mutant also showed only a mild increase in IC_{50} for ruxolitinib and no resistance to SAR302503, in contrast to the strong kinase inhibitor resistance conferred by gatekeeper mutations in several other kinases.[10] These results indicate that mutations in the gatekeeper residue are not expected to occur in patients treated with ruxolitinib or SAR302503. In contrast, mutations Y931C and G935R found in *in vitro* screens conferred strong resistance to ruxolitinib.[15] Based on the proposed binding mode (Figure 1c), the aromatic side chain of Y931 enhances the binding of the double-ring

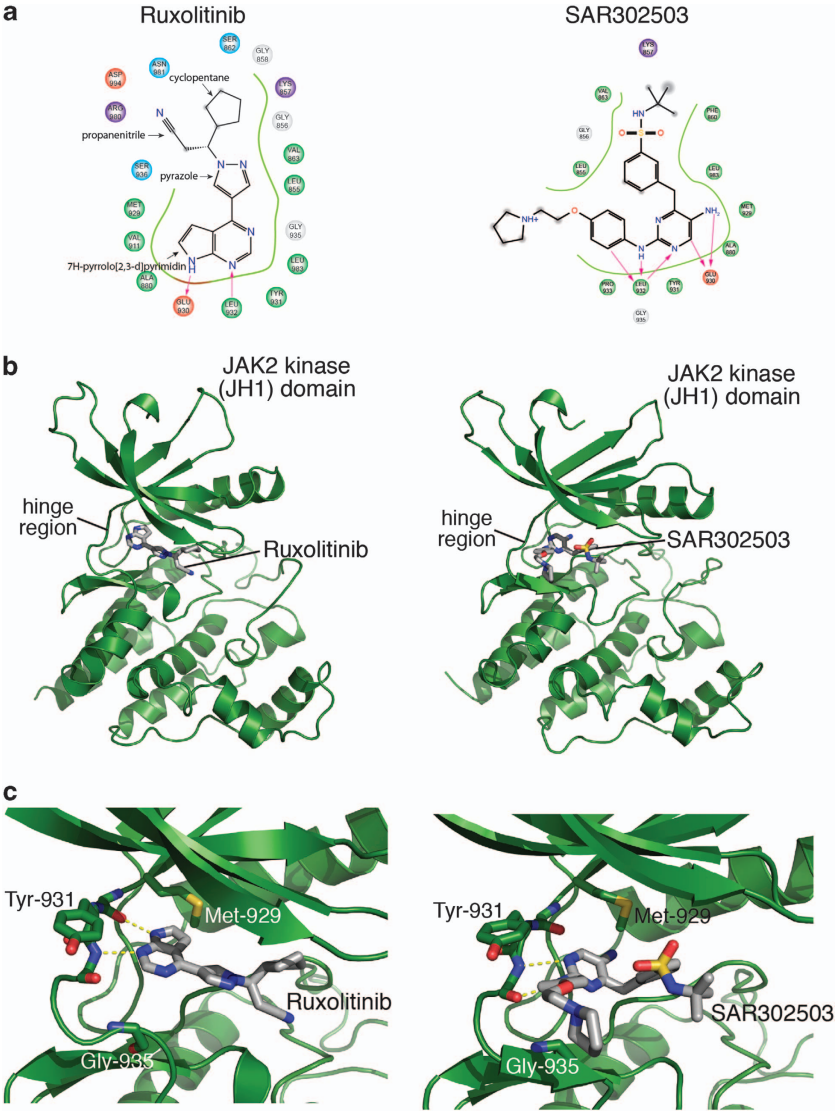

Figure 1. The predicted binding mode of ruxolitinib (left) and SAR302503 (right) to the JAK2 kinase domain. (**a**) Most populated binding mode of ruxolitinib (left) and SAR302503 (right) in the MD simulations. These two-dimensional plots were prepared with Ligplot.[17] They show the JAK2 residues in van der Waals contact with the drugs (green, cyan, blue, red and white circles for hydrophobic, polar, basic, acidic and glycine residues, respectively), the intermolecular hydrogen bonds (magenta arrows) and the atoms of the drugs exposed to solvent (gray circles). Ring systems and functional groups of ruxolitinib that are mentioned in the text are labeled. (**b**) Cartoon representation of the JAK2 kinase domain bound to ruxolitinib (left) and SAR302503 (right). As in panel (**a**), the most populated binding mode of the drugs in the MD simulations is shown. (**c**) Detailed view of the drug-binding sites. Critical hydrogen bonds to the hinge region are indicated by a yellow dotted line. Met-929 (gatekeeper residue) as well as Tyr-931 and Gly-935 that were shown to render JAK2 resistant to ruxolitinib and SAR302503 upon mutation, are shown as sticks. A detailed description of the employed methods and results can be found in Supplementary Data.

system in ruxolitinib by shielding the key hydrogen bonds with the hinge region (E930 and L932) from aqueous surroundings, which are disrupted upon Y931C mutation. The G935R mutation introduces a bulky side chain that may sterically hinder the binding of ruxolitinib. Importantly, these two mutants are also cross-resistant to SAR302503,[15] in line with the role of Y931 in stabilizing the binding and the steric conflicts of a bulky side chain at position 935 (Figure 1c).

In summary, we present a comprehensive survey of the near-kinome-wide specificity of ruxolitinib and SAR302503, which reveals potentially clinically relevant off-targets. Furthermore, our MD simulations suggest possible binding modes of both inhibitors. The binding modes explain the mechanism-of-action of resistance-causing point mutations that were observed *in vitro* and serves as a template to interpret mutations that may arise in patients treated with JAK2 inhibitors.

CONFLICT OF INTEREST

The authors declare no conflict of interest.

ACKNOWLEDGEMENTS

This work was supported by the ISREC Foundation (grant to OH and SG), the Swiss National Science Foundation (grant to AC) and the Olga Mayenfisch Foundation. The MD simulations were carried out on the Schroedinger computer cluster of the University of Zurich.

T Zhou[1], S Georgeon[2], R Moser[3], DJ Moore[3], A Caflisch[1,4] and O Hantschel[2,4]
[1]*Department of Biochemistry, University of Zürich, Zürich, Switzerland;*
[2]*Swiss Institute for Experimental Cancer Research, School of Life Sciences, École polytechnique fédérale de Lausanne, Lausanne, Switzerland and*
[3]*Brain Mind Institute, School of Life Sciences, École polytechnique fédérale de Lausanne, Lausanne, Switzerland*
[4]*Joint senior authors in this study.*
E-mail: caflisch@bioc.uzh.ch or oliver.hantschel@epfl.ch

REFERENCES

1 Skoda R. The genetic basis of myeloproliferative disorders. *Hematology AmSoc Hematol Educ Program* 2007: 1–10.
2 Tefferi A, Vainchenker W. Myeloproliferative neoplasms: molecular pathophysiology, essential clinical understanding, and treatment strategies. *J Clin Oncol* 2011; **29**: 573–582.
3 Pardanani A, Vannucchi AM, Passamonti F, Cervantes F, Barbui T, Tefferi A. JAK inhibitor therapy for myelofibrosis: critical assessment of value and limitations. *Leukemia* 2011; **25**: 218–225.
4 Harrison C, Kiladjian JJ, Al-Ali HK, Gisslinger H, Waltzman R, Stalbovskaya V *et al.* JAK inhibition with ruxolitinib versus best available therapy for myelofibrosis. *N Engl J Med* 2012; **366**: 787–798.
5 Verstovsek S, Mesa RA, Gotlib J, Levy RS, Gupta V, DiPersio JF *et al.* A double-blind, placebo-controlled trial of ruxolitinib for myelofibrosis. *N Engl J Med* 2012; **366**: 799–807.
6 Pardanani A, Gotlib JR, Jamieson C, Cortes JE, Talpaz M, Stone RM *et al.* Safety and efficacy of TG101348, a selective JAK2 inhibitor, in myelofibrosis. *J Clin Oncol* 2011; **29**: 789–796.
7 Geyer HL, Tibes R, Mesa RA. JAK2 inhibitors and their impact in myeloproliferative neoplasms. *Hematology* 2012; **17**(Suppl 1): S129–S132.
8 Quintás-Cardama A, Vaddi K, Liu P, Manshouri T, Li J, Scherle PA *et al.* Preclinical characterization of the selective JAK1/2 inhibitor INCB018424: therapeutic implications for the treatment of myeloproliferative neoplasms. *Blood* 2010; **115**: 3109–3117.
9 Wernig G, Kharas MG, Okabe R, Moore SA, Leeman DS, Cullen DE *et al.* Efficacy of TG101348, a selective JAK2 inhibitor, in treatment of a murine model of JAK2V617F-induced polycythemia vera. *Cancer Cell* 2008; **13**: 311–320.
10 Lamontanara AJ, Gencer EB, Kuzyk O, Hantschel O. Mechanisms of resistance to BCR-ABL and other kinase inhibitors. *Biochim Biophys Acta* 2013; **1834**(7): 1449–1459.
11 Hantschel O, Warsch W, Eckelhart E, Kaupe I, Grebien F, Wagner K-U *et al.* BCR-ABL uncouples canonical JAK2-STAT5 signaling in chronic myeloid leukemia. *Nat Chem Biol* 2012; **8**: 285–293.
12 Rudenko IN, Chia R, Cookson MR. Is inhibition of kinase activity the only therapeutic strategy for LRRK2-associated Parkinson's disease? *BMC Med* 2012; **10**: 20.
13 Lafleur K, Dong J, Huang D, Caflisch A, Nevado C. Optimization of inhibitors of the tyrosine kinase EphB4. 2. Cellular potency improvement and binding mode validation by X-ray crystallography. *J Med Chem* 2013; **56**: 84–96.
14 Liu Y, Gray NS. Rational design of inhibitors that bind to inactive kinase conformations. *Nat Chem Biol* 2006; **2**: 358–364.
15 Deshpande A, Reddy MM, Schade GOM, Ray A, Chowdary TK, Griffin JD *et al.* Kinase domain mutations confer resistance to novel inhibitors targeting JAK2V617F in myeloproliferative neoplasms. *Leukemia* 2012; **26**: 708–715.
16 Hantschel O, Rix U, Schmidt U, Burckstummer T, Kneidinger M, Schutze G *et al.* The Btk tyrosine kinase is a major target of the Bcr-Abl inhibitor dasatinib. *Proc Natl Acad Sci USA* 2007; **104**: 13283–13288.
17 Wallace AC, Laskowski RA, Thornton JM. LIGPLOT: a program to generate schematic diagrams of protein-ligand interactions. *Protein Eng* 1995; **8**: 127–134.

Supplementary Information accompanies this paper on the Leukemia website (http://www.nature.com/leu)